Passive Moisture Sensor Based on Conductive and Water-Soluble Yarns

Xiaochen Chen, Han He, Meinan Gou, Yunshan Yang, Lauri Sydänheimo, Leena Ukkonen, Johanna Virkki

***Abstract*—In this paper, we establish a new type of passive ultra-high-frequency (UHF) radio frequency identification (RFID) technology-based moisture sensor. The sensor system consists of a sensor tag and a reference tag to indicate exposure to moisture. The sensor tag is fabricated on a cotton substrate from conductive silver yarn and water-soluble polyvinyl alcohol (PVA) yarn. When the sensor is exposed to water, the PVA yarn will melt, which causes a permanent change to the tag antenna body and to the wireless performance of the sensor tag. By measuring the backscattered power strength difference, ΔP, the presence of moisture can be detected and recorded. When ΔP is below 0, the sensor system shows that it has been in a highly moist condition. Our PVA-based moisture-sensing system can provide cost-effective and maintenance-free monitoring of moisture exposure for versatile application fields.**

***Index Terms*— embroidery, moisture sensor, passive UHF RFID technology, polyvinyl alcohol, wireless sensor, zero-energy sensor.**

I. Introduction

Polyvinyl alcohol (PVA) is a water-soluble synthetic polymer. It is commonly used in papermaking, for example, or in textiles, as well as in a variety of coatings. It can be obtained in the form of solid beads or as solutions in water [1, 2]. The use of PVA has been studied in various application fields [3], such as adhesive materials [4], transient devices [5], and drug delivery systems [6]. PVA's environment-friendly qualities make it a particularly interesting material. Once PVA is dissolved into water, a specific microorganism will cause it to degrade. Thus, when treated with an activated sludge, PVA decomposes into water and carbon dioxide [7]. In addition to its biocompatibility and biodegradability, PVA's steerable water-solubility [8] and excellent dielectric properties [9] have also made it a promising material for substrates or as a supporting material for electronic devices.

Wireless electronic components are rapidly becoming an integral part of day-to-day life. Sensing and localization systems, and many other wearable devices [10-15] are increasingly prevalent in today's society. In this context, passive radio frequency identification (RFID) technology benefits from its wireless, battery-less, and thus maintenance-free features. No surprise, therefore, that it is attracting keen scrutiny as it is recognized as one of the key components of the wireless world [16-19]. Many studies have proved that RFID tags can show detectable changes in wireless performance. These can be caused by, for example, strain [20-22], temperature [23, 25], or moisture [25-29]. It has also been shown that utilising a reference tag in the sensor system will greatly help to increase the accuracy of any practical sensing system for strain and compression [30, 31].

In this paper, we explore the advantages of combining the great material properties of PVA with passive RFID technology. We present a passive moisture-sensing system for the global ultra-high frequency (UHF) RFID frequency band. The device is fabricated from water-soluble PVA yarn and conductive silver-coated yarn on a cotton substrate. To the best of our knowledge, this is the first study utilizing PVA as a sensing material in a passive, wireless moisture-sensor. This novel sensor system consists simply of a sensor tag and a reference tag, yet it can detect if moisture has been present on the sensor tag, by permanently changing the wireless performance of the sensor tag. This low-cost solution would not only be useful in wearable health-monitoring applications, but could be useful in detecting the moisture-exposure of any number of moisture-sensitive items, as well as dried foodstuff.

II. Material Study

The moisture-sensing material was a water-soluble PVA yarn as shown in Table 1. The first tests were to study the solubility of the yarn in different liquids. We looked at the melting time of the yarn over a temperature range from 22 °C (room temperature) to 50 °C. The results are shown in Table. 2. We also looked at the effects of adding sugar and salt to room-temperature water. These results are shown in Table 3. In each case, we tested 10 samples and calculated the average and

Table. 1. Technical data of PVA yarn.

Specifications	
Actual Count	20 s
Type of Fiber Blend	100 % PVA Fiber
Strength Coefficient of Variation %	9.2

This research was funded by the Academy of Finland (294534) and Jane and Aatos Erkko Foundation.

Xiaochen Chen, Han He, Lauri Sydänheimo, Leena Ukkonen, Johanna Virkki are with the Faculty of Medicine and Health Technology, Tampere University, Tampere 33720, Finland (e-mail: xiaochen.chen@tuni.fi; han.he@tuni.fi; zahangir.khan@tuni.fi; lauri.sydanheimo@tuni.fi; leena.ukonen@tuni.fi; johanna.virkki@tuni.fi)

Meinan Gou, Yunshan Yang are with Department of Electrical Engineering, City University of Hong Kong, Hong Kong, China (e-mail: meinangou2-c@my.cityu.edu.hk; yunshyang3-c@my.cityu.edu.hk)

Table 2. Melting time in different water temperatures.

Temperature (˚C)	Time (s)	Standard Dev.
22	20.2	1.24
26	9.76	1.56
30	3.76	0.46
40	3.37	0.35
50	2.35	0.04

Table 3. Melting time in different water solutions (in 22 °C).

Concentration	Salt Solution		Sugar Solution	
g/L	Time (s)	Stand. Dev.	Time (s)	Stand. Dev.
0	19.39	0.934	16.5	0.19
50	19.84	0.934	18.2	0.81
100	21.73	1.261	18.6	0.37
200	59.92	3.089	18.68	0.86
300	163.88	8.722	19.8	1.08

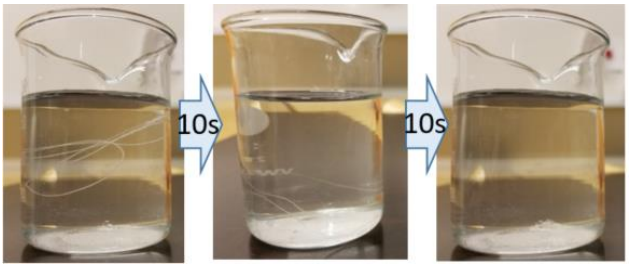

Fig. 1. PVA yarn dissolving into water in 20 seconds (in a room temperature).

standard deviation values of the melting time. As can be seen from the results, the PVA-based yarn dissolved completely in all these conditions. The test results also clearly show that a higher temperature significantly speeded up the melting process. On the other hand, a higher salt concentration clearly decreased the melting rate. However, sugar only seemed to have a slight effect on the melting time.

The photographs in Fig. 1. clearly show the speed of the process as the PVA yarn melts in room-temperature water. The yarn quickly becomes translucent before dissolving away completely in just 20 seconds.

III. Sensor System Design and Fabrication

A diagram of the structure and size of the sensor and reference tag antennae are shown in Fig. 2. The RFID integrated circuit (IC) component (NXP UCODE G2iL series RFID IC) shown in Fig. 3 is the one used in our study. The antenna of the sensor tag was made from conductive silver yarn (Shieldex multifilament thread 110f34 dtex 2-ply HC) and water soluble PVA yarn (100 % PVA fiber). The DC linear resistivity of the conductive yarn was 500±100 Ω/m, and it was approximately 0.16 mm in diameter. The sheet resistance was measured as being around 0.2 ohm/square. The sensor tag antenna was embroidered onto a plain cotton fabric substrate. Part A of the antenna (as shown in Figure 4) was embroidered onto the substrate first. Figure 4 also shows how the RFID IC component was attached by its copper pads using the same conductive yarn. Next, the water-soluble PVA yarn was embroidered on the corners of Part A. Finally, Part B of the antenna (as shown in Fig. 4) was embroidered on top of the PVA yarn at the corners of Part A. The PVA yarn was thus used to isolate parts A and B of the antenna. Consequently, when the sensor tag is dipped into water, the PVA yarn melts, allowing the two parts of the antenna to connect, as shown in Fig. 5. As the conductive body of the antenna is thus extended, the wireless performance of the tag antenna changes, i.e. the tag acts as a moisture sensor. It must here be noted, of course, that the moisture in the cotton cloth may change the conductivity of the substrate, which may then influence the sensor's wireless performance. This is

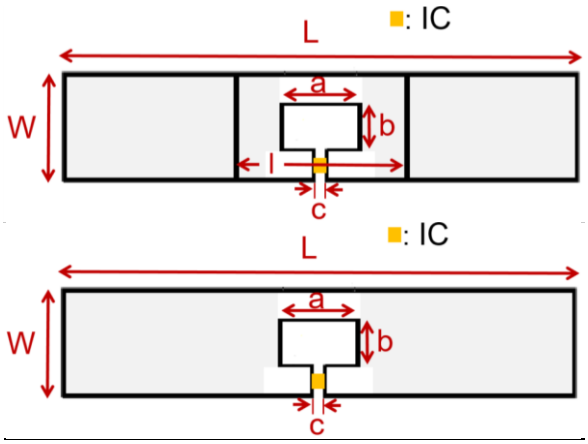

L	W	a	b	c	l
100	20	14.3	8.125	2	30

Fig. 2. Structure and size of sensor tag (top) and reference tag (bottom), unit in mm.

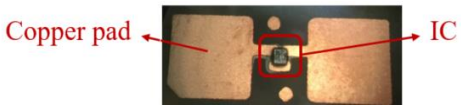

Fig. 3 RFID IC component used in this study.

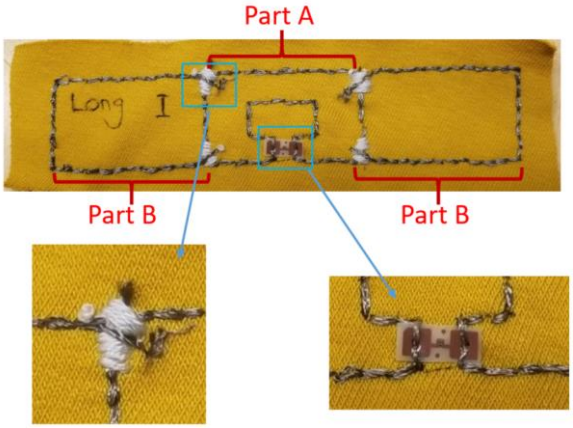

Fig. 4. Ready-made sensor tag with water soluble yarn separating Part A and Part B (left) and embroidered antenna-IC interconnection (right).

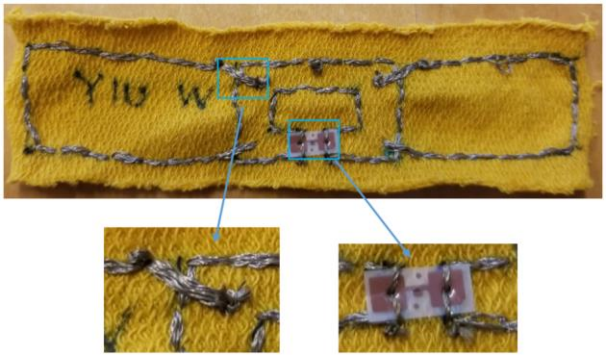

Fig. 5. Sensor tag after exposure to water.

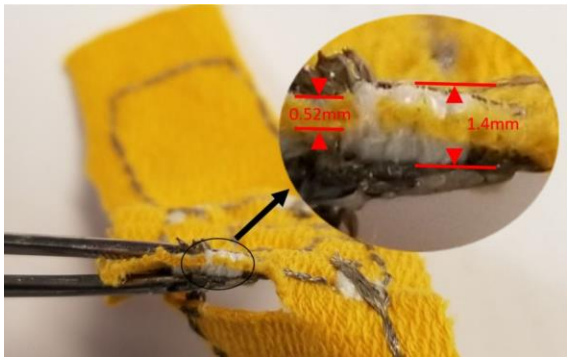

Fig 6. Cross-section of the PVA yarn part on the sensor tag.


Fig. 7. The ready-made comparison tag.


Fig. 8. Ready-made electro-textile reference tag.

especially critical in the area around the IC, as the higher conductivity of the substrate may short-circuit the IC. Thus, after exposure to moisture, the whole system has to be dried out again for optimum performance.

The PVA yarn itself is of great importance. A close-up of the PVA yarn part of the sensor tag is shown in Fig 6. The diameter of a single PVA thread is 0.1 mm. Nevertheless, after embroidery, the total thickness of the PVA part is 1.4 mm, while the initial thickness of the substrate was 0.52 mm. It seems likely that the melting time of the water-soluble yarn will increase as the thickness of the embroidered yarn increases. In this study, the water-soluble yarn was embroidered onto the substrate as thinly as possible in order to minimise the PVA yarn's melting time. This factor must be accounted for in any similar tests.

Furthermore, a comparison tag group was fabricated, as shown in Fig 7. These tag antennas (Part A and Part B) used the same cotton substrate and conductive yarn, but without any PVA yarn separating the two antenna parts.

Our reference tag antenna design is widely used in this field, (as in [29] for example) and is known for its good wireless performance. The reference tag antenna (shown in Fig. 8) was fabricated using nickel-plated Less EMF Shieldit Super Fabric (Cat. #A1220) as the electro-textile conductor. It was cut with a laser cutter (Epilog Fusion Laser Model 13000). Conductive silver epoxy (Circuit Works CW2400) was used to connect the same RFID IC as used for the sensor tags.

In this sensor system, the changed wireless response of the sensor tag is used to detect exposure to moisture, while the wireless performance of the reference tag remains stable after being dipped into the water. The backscattered signals of passive RFID tags are noisy, unstable, and strongly affected by the environment. By including the reference tag, the influence of the environment can be minimized.

IV. Sensor Measurements

A. Sensor functionality testing

Sensor tag functionality was firstly tested in an anechoic chamber with Voyantic Tagformance RFID measurement system. All the measurements were conducted with the sensor tag suspended on a foam structure (as shown in Fig. 9). The sensor tag was immersed in water for a half an hour at room temperature, after which the water-soluble yarn had totally dissolved and thus Part A and Part B of the antenna were connected.

The wireless channel from the reader antenna to the location of the sensor tag was first measured using a system reference tag with known properties. The lowest continuous-wave transmission power (threshold power: P_{th}) of the sensor tag was recorded. As has been detailed in [32], this enabled us to estimate the attainable read range of the sensor tag (d_{tag}) versus frequency from:

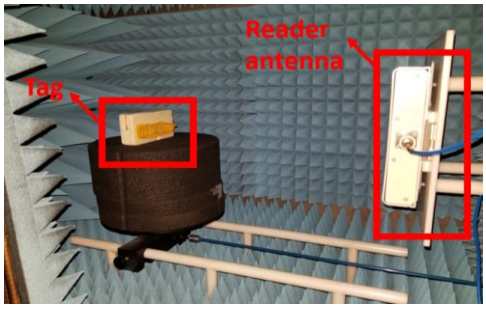

Fig. 9. Sensor tag measurement setup in an anechoic chamber.

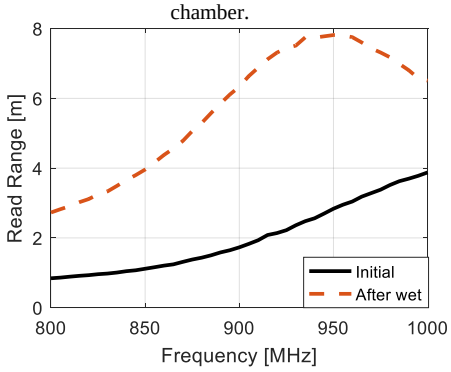

Fig. 10. Read range of a sensor tag initially and after in water for 30 minutes + drying for 24 hours.

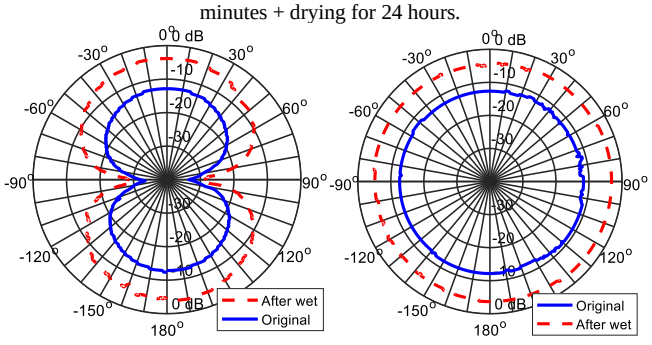

Fig. 11. Radiation pattern of a sensor tag initially and after in water for 30 minutes + drying for 24 hours: E-plane (left) and H-plane (right).

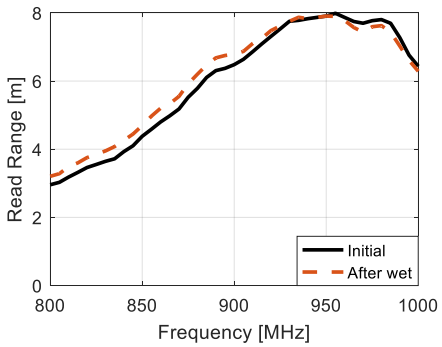

Fig. 12. Read range of a comparison tag initially and after in water for 30 minutes + drying for 24 hours.

$$d_{tag} = \frac{\lambda}{4\pi}\sqrt{\frac{EIRP}{\Lambda}\frac{P_{th^*}}{P_{th}}}, \quad (1)$$

where λ is the wavelength transmitted from the reader antenna, P_{th} is the measured threshold power of the tag, Λ is a known constant describing the sensitivity of the system reference tag, P_{th^*} is the measured threshold power of the system reference tag, and *EIRP* is the equivalent isotropic radiated power (3.28 W, according to the emission limit in Europe).

The realized gain of the sensor tag was then analyzed using the path-loss measurement data from the measurement system. The realized gain (G_r) takes into account the antenna–IC impedance matching and can be calculated as:

$$G_r = \frac{P_{IC,TS}}{L_{fwd} \times P_{th}} \quad (2)$$

where $P_{IC,TS}$ is the tag IC sensitivity and L_{fwd} is the measured forward losses.

As shown in Fig. 10, the attainable read range of the sensor tag at the initial condition was around 2 meters from 866 MHz to 915 MHz, a frequency range that covers most RFID operation frequencies globally. After being immersed in water for 30 minutes and then dried for 24 hours, the read range of the sensor tang was around 5-7 meters from 866 MHz to 915 MHz. The significant increase in the read range was caused by the melting of the PVA yarn, connecting Parts A and B of the antenna, and thus extending the antenna body. The measured E-plane and H-plane radiation patterns, shown in Fig. 11, also increased after the sensor tag got wet and dry again. Altogether 4 sensor tags were tested and they all showed similar performance.

The comparison tags were also tested, initially in the anechoic chamber then after being submerged in water for 30 minutes and drying for 24 hours. Their read range results are shown in Fig. 12. After the sensor tag's exposure to water, the water-soluble yarn melted. The read range of the sensor tag after exposure to water was similar to the initial read range of the comparison tag (which was fabricated without the water-soluble yarn). Furthermore, the read range of the comparison tag did not change after exposure to moisture. Thus, this test verified that the change of the wireless performance of the sensor tags was caused by the dissolving PVA structure, and not by, for example, changes in the cotton substrate or antenna-IC impedance matching. All 4 of the comparison tags were tested, and they all showed similar performance.

B. Practical sensor testing

In actual sensor testing, a Thing Magic M6 RFID reader was used for recording the backscattered powers. In the sensor system (shown in Fig. 13), the reference tag is located orthogonally, at a distance of 5 cm from the sensor tag, since the signal from the reader to the closely spaced tags travels approximately through the same channel. As the reference tag is placed next to the sensor tag, it always has the same distance to the reader antenna as the sensor tag. The 3 dB azimuth beamwidth and 3 dB elevation beamwidth of the reader antenna are 65˚. Thus, the orientation of the reader antenna affected the transmitted power, and then influenced the read range of the sensor and reference tags. The sensor platform was measured at the antenna front-center area, as well as at a 30˚ angle from the antenna center, to test the system performance from different angles.

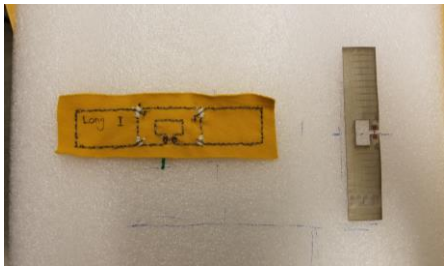

Fig. 13. Configuration of a sensor tag and a reference tag.

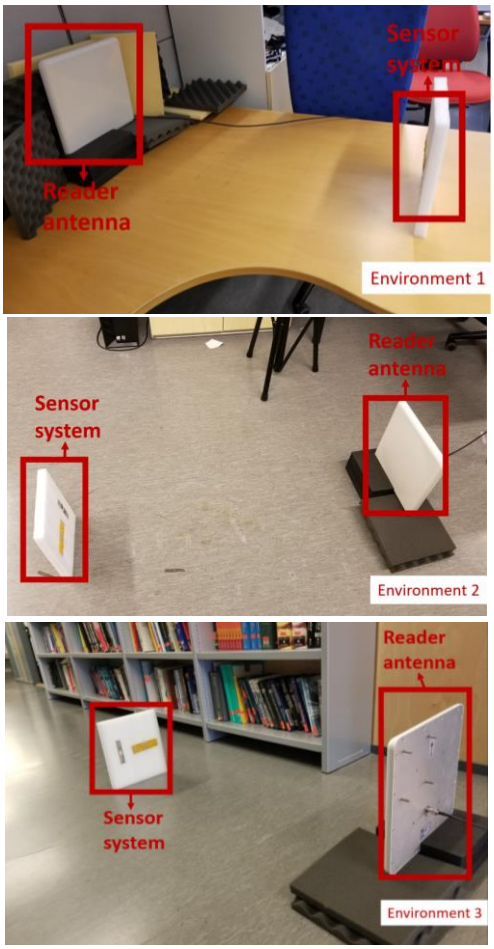

Fig. 14. Practical measurements in an office (environments 1 and 2) and in a corridor (environment 3).

Table 4. Backscattered power of original sensor tag (Sens. or) and reference tag (Ref. or) before dipped into water, as well as sensor (Sens. 0.9, Sens. 1.6) and reference tag (Ref. 0.9, Ref. 1.6) once re-dry in environment 1 at 0.9 meters and 1.6 meters, respectively, unit in dBm.

Time(s)	0.1	0.2	0.3	0.4	0.5	0.6	0.7	0.8	0.9	1
Sens. or	-62	-63	-63	-63	-62	-63	-63	-63	-63	-62
Ref. or	-51	-51	-51	-52	-51	-52	-52	-51	-52	-51
Sens.0.9	-48	-48	-48	-48	-48	-48	-49	-48	-48	-49
Ref. 0.9	-51	-51	-51	-51	-51	-51	-51	-51	-51	-51
Sens.1.6	-63	-62	-62	-63	-64	-63	-63	-64	-64	-64
Ref. 1.6	-63	-63	-63	-64	-63	-63	-63	-64	-64	-64

Table 5. Backscattered power of original sensor tag (Sens. or) and reference tag (Ref. or) before dipped into water, as well as sensor (Sens. 0.9, Sens. 1.6) and reference tag (Ref. 0.9, Ref. 2.1) once re-dry in environment 2 at 0.9 meters and 2.1 meters, respectively, unit in dBm.

Time(s)	0.1	0.2	0.3	0.4	0.5	0.6	0.7	0.8	0.9	1
Sens. or	-61	-62	-62	-62	-61	-62	-62	-62	-62	-61
Ref. or	-53	-53	-53	-53	-53	-53	-52	-52	-53	-53
Sens.0.9	-48	-48	-48	-48	-48	-48	-48	-48	-48	-48
Ref. 0.9	-51	-51	-51	-51	-51	-52	-51	-51	-51	-51
Sens.2.1	-62	-61	-62	-62	-61	-61	-61	-61	-62	-61
Ref. 2.1	-70	-71	-71	-71	-69	-70	-70	-69	-69	-70

Table 6. Backscattered power of original sensor tag (Sens. or) and reference tag (Ref. or) before dipped into water, as well as sensor (Sens. 0.9, Sens. 2.2) and reference tag (Ref. 0.9, Ref. 2.2) once re-dry in environment 3 at 0.9 meters and 2.2 meters, respectively, unit in dBm.

Time(s)	0.1	0.2	0.3	0.4	0.5	0.6	0.7	0.8	0.9	1
Sens. or	-62	-63	-62	-63	-62	-62	-63	-63	-63	-62
Ref. or	-54	-53	-54	-53	-54	-54	-54	-54	-54	-53
Sens.0.9	-47	-47	-47	-47	-47	-47	-47	-47	-47	-47
Ref. 0.9	-52	-52	-53	-52	-52	-52	-52	-52	-52	-52
Sens.2.2	-63	-62	-62	-61	-62	-62	-62	-62	-62	-62
Ref. 2.2	-67	-67	-66	-67	-66	-66	-66	-66	-66	-67

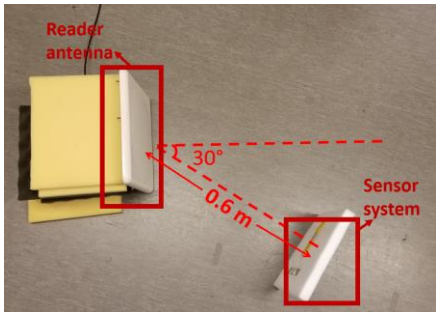

Fig. 15. The measurement of the sensor platform at a 30˚ angle from the antenna center.

Table 7. Backscattered power in the 30˚ orientation test of original sensor tag (Sens. or.) and reference tag (Ref. or.) before dipped into water, as well as the sensor tag (Sens. aft.) and reference tag (Ref. aft.) once re-dry, respectively, unit in dBm.

Time(s)	0.1	0.2	0.3	0.4	0.5	0.6	0.7	0.8	0.9	1
Sens.or.	-64	-64	-63	-64	-64	-64	-64	-64	-64	-64
Ref. or.	-57	-57	-57	-57	-57	-57	-57	-57	-57	-57
Sens.aft.	-51	-51	-51	-51	-51	-51	-51	-51	-51	-51
Ref. aft.	-57	-57	-57	-57	-57	-57	-57	-57	-57	-57

The sensor system was tested in three different environments, (twice in an office and once in a corridor, as shown in Fig. 14). The transmitted power at 866 MHz was 28 dBm and the sensor system was first measured at a distance of 0.9 cm. The backscattered powers of both tags were recorded. After the sensor tag was exposed to water and dried again, the read range of the sensor tag increased in every test condition. According to the measurement results, the sensor tag could be measured from distances of 1.6, 2.1 and 2.2 meters (the longest detected range in the three testing environments) respectively.

The measurement results from testing environments 1-3 are shown in Tables 4-6, respectively. Since the backscattered power of both the reference tag and the sensor tag was stable during the measurements, the tables present 10 recordings done in 1 second. As can be seen, the backscattered powers of the reference tags were initially higher than those of the sensor tags. However, after the sensor system had been exposed to water and got dry again, the backscattered power of the sensor tag became almost equal to, or even higher, than the reference tag for each distance and test condition.

As shown in Fig. 15, the sensor platform was also tested at a 30˚ angle to the centre of the antenna. As the sensor platform was not located front-center of the reader antenna, there was a decrease in the transmitted power. In this case, the maximum detection range was 0.6 meters. The full measurement results are shown in Table. 7.

In this study, we derive the water exposure from the value ΔP of the difference in the strength of the backscattered power, defined as $\Delta P = P_{ref} - P_{sns}$, where P_{sns} and P_{ref} are the backscattered power strengths from the sensor tag and the reference tag, respectively. As shown in Fig. 13, ΔP was only above 0 in the initial condition, which meant that the backscattered power of the reference tag was higher than that of the sensor tag in all three of the different environments. After the sensor tag got exposed to water, the backscattered power of the system was measured from different distances in each environment.

As shown in Fig. 16, for the front-center measurements, ΔP changed to below 0 in all 3 environments, and from all distances. Thus, these preliminary results show that this sensor system could be used to sense exposure to water using the ΔP parameter.

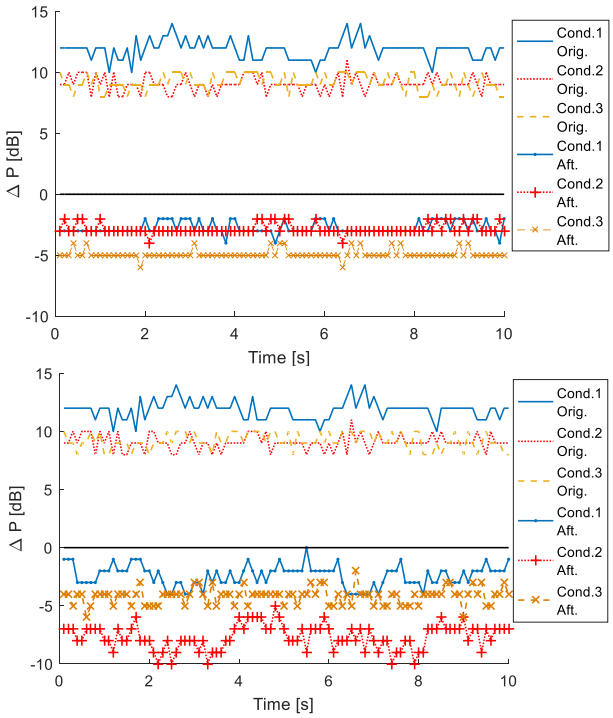

Fig. 16. ΔP at a distance of 0.9 meters (top) and furthest possible distance of each testing environment (bottom).

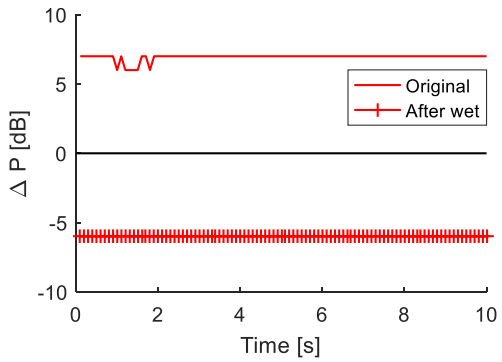

Fig. 17. Δ*P* at distance of 0.6 meters and 30˚ from front-center direction.

The calculated *ΔP* at 0.6 meters and 30˚ from the front-center direction is shown in Fig. 17. In these results, *ΔP* had the same regulation as with the front-center direction measurements: once the system had got wet and then got dry again, *ΔP* could be measured as being less than 0. Thus, the system still works when the sensor is placed at a 30˚ angle to the centre of the reader antenna center, it is just that the read range has decreased. Interestingly, in this position *ΔP* was much more stable than it was for the front-center measurements. This may be caused by less interference from the wireless system, as the distance between the sensor platform and the reader antenna is shorter, in this case 0.6 meters.

In addition, 3 different sensor tags were tested in ground conditions to verify the stability of this sensor system design. The measurements were taken from the front at a distance of 0.9 meters. The calculated *ΔP* and standard deviation (σ) over 10 seconds are shown in Table 8. Consequently, all the $\Delta P_{2\text{-}4}$ values were above 0 initially, but changed to less than 0 for all these tests after being immersed in water, thus demonstrating that our system is reliable with different sensor tags.

Table 8. The measurement results for three different sensor tags.

	Original condition		After dipped into water	
	Average	σ	Average	σ
ΔP_2	8.98	0.6814	-14.78	0.4399
ΔP_3	1.15	0.5871	-6.93	0.3555
ΔP_4	5.70	0.5946	-2.83	0.4277

In any practical application of this technology, such as in a frozen-food transportation chain, any cargo with this sensor tag system may be initially scanned in one environment, where the Δ*P* value should be above 0. At the end of the transportation chain, in a different environment, the value of ΔP should keep below 0 only if it has melted at some point . In order to make sure that the system can accurately indicate the exposure to water in different environments, it is essential to first verify the sensor's performance in multiple conditions. In this study, we have tested the system in three different environments, the results of all of which support the use of this sensor system.

V. Conclusions

In this paper, we have presented the design, fabrication, wireless evaluation, and practical testing of a new type of passive moisture-sensor system. The sensor is fabricated on a cotton substrate using water-soluble PVA yarn and conductive silver yarn. After being immersed in water for half an hour, the PVA yarn dissolves, permanently changing the structure of the sensor tag antenna. By measuring the backscattered power strength difference, *ΔP*, the exposure to moisture can be detected. When *ΔP* is below 0, the sensor system shows that it has been in a highly moist condition.

This sensor system is flexible and lightweight and is cheap and easy to make. Due to the wirelessly accessible permanent indication of moisture exposure, it could be utilized as in the above example for a frozen food supply chain, or in wearable applications related to health monitoring.

To the best of our knowledge, this is the first presentation of a passive wireless sensing system based on a PVA material. After these encouraging preliminary results, further testing will be carried out with a larger range of samples. The next steps will also include combining different types of temperature-sensitive water-soluble yarns. The effects of salt on the sensor's performance will also be studied further.

REFERENCES

[1] M. L. Hallensleben, "Polyvinyl compounds, others," Ullmann's Encyclopedia of Industrial Chemistry, Weinheim: Wiley-VCH, 2000.

[2] X. Tang, S. Alavi, "Recent advances in starch, polyvinyl alcohol based polymer blends, nanocomposites and their biodegradability," Carbohydrate Polymers, vol. 85, no. 1, pp. 7-16, 2011.

[3] F. Xu, H. Zhang, L. Jin, Y. Li, J. Li, G. Gan, M. Wei, M. Li and Y. Liao, "Controllably degradable transient electronic antennas based on water-soluble PVA/TiO2 films," Journal of Materials Science, vol. 53, no. 4, pp. 2638-2647, 2018.

[4] Y. Mu, X. Wan, "Simple but strong: A mussel-inspired hot curing adhesive based on polyvinyl alcohol backbone," Macromolecular Rapid Communications, vol. 37, no. 6, pp. 545-550, 2016.

[5] L. Yin, X. Huang, H. Xu, Y. Zhang, J. Lam, J. Cheng and J. A. Rogers, "Materials, designs, and operational characteristics for fully biodegradable primary batteries," Advanced Materials, vol. 26, no. 23, pp. 3879-3884, Mar. 2014.

[6] X. Wang, T. Yucel, Q. Lu, X. Hu and D. L. Kaplan, "Silk nanospheres and microspheres from silk/PVA blend films for drug delivery," Biomaterials, vol. 31, no. 6, pp. 1025–1035, Feb. 2011.

[7] Plasticisrubbish, [accessed on 21.11.2019]. Available at: http://plasticisrubbish.com/2014/07/12/whitby-goths-and-cocoa/, 12.7.2014.

[8] H. Acar, S. Cinar, M. Thunga, M. R. Kessler, N. Hashemi and R. Montazami, "Study of physically transient insulating materials as a potential platform for transient electronics and bioelectronics," Advanced Functional Materials, vol. 24, no. 26, pp. 4135–4143, 2014.

[9] V. Frosini, E. Butta and M. Calamia, "Dielectric behavior of some polar high polymers at ultra-high frequencies (microwaves)," Journal of Applied Polymer Science, vol. 11, no. 4, pp. 527–551, Apr. 1967.

[10] T. Kaufmann, D. C. Ranasinghe, M. Zhou and C. Fumeaux, "Wearable quarter-wave folded microstrip antenna for passive UHF RFID applications," International Journal of Antennas and Propagation, Article ID 129839, 2013.

[11] O. O. Rakibet, C. V. Rumens, J. C. Batchelor and S. J. Holder, "Epidermal passive RFID strain sensor for assisted technologies," IEEE Antennas and Wireless Propagation Letters, vol. 13, 2014.

[12] C. Occhiuzzi, C. Vallese, S. Amendola, S. Manzari and G. Marrocco, "NIGHT-Care: A Passive RFID system for remote monitoring and control

of overnight living environment," Procedia Computer Science, vol. 32, pp. 190-197, 2014.

[13] D. Patron, W. Mongan, T. P. Kurzweg, A. Fontecchio, G. Dion, E. K. Anday, and K. R. Dandekar, "On the use of knitted antennas and inductively coupled RFID tags for wearable applications," IEEE Transactions on Biomedical Circuits and Systems, vol. 10, no. 6, pp. 1047-1057, 2016.

[14] W. Wang, R. Owyeung, A. Sadeqi and S. Sonkusale, "Single Event Recording of Temperature and Tilt Using Liquid Metal With RFID Tags," in IEEE Sensors Journal, vol. 20, no. 6, pp. 3249-3256, 15 March15, 2020.

[15] S. Kim, Y. Kawahara, A. Georgiadis, A. Collado and M. M. Tentzeris, "Low-Cost Inkjet-Printed Fully Passive RFID Tags for Calibration-Free Capacitive/Haptic Sensor Applications," in IEEE Sensors Journal, vol. 15, no. 6, pp. 3135-3145, June 2015.

[16] T. Leng, X. Huang, K. H. Chang, J. Chen, M. A. Abdalla, and Z. Hu, "Graphene nanoflakes printed flexible meandered-line dipole antenna on paper substrate for low-cost RFID and sensing applications," IEEE Antennas and Wireless Propagation Letters, vol. 15, pp. 1565-1568, 2016.

[17] Y. Feng, L. Xie, Q. Chen, and L. R. Zheng, "Low-cost printed chipless RFID humidity sensor tag for intelligent packaging," IEEE Sensors Journal, vol. 15, no. 6, pp. 3201-3208, 2015.

[18] D. Shuaib, L. Ukkonen, J. Virkki, and S. Merilampi, "The possibilities of embroidered passive UHF RFID textile tags as wearable moisture sensors," in Proceedings of IEEE 5th International Conference on Serious Games and Applications for Health (SeGAH), Perth, WA, Australia, pp. 1-5, 2nd-4th, April, 2017.

[19] S. Merilampi, T. Björninen, L. Ukkonen, P. Ruuskanen, and L. Sydänheimo, "Embedded wireless strain sensors based on printed RFID tag," Sensor Review, vol. 31, no.1, pp. 32-40, 2011.

[20] S. Caizzone, C. Occhiuzzi, and G. Marrocco, "Multi-chip RFID antenna integrating shape-memory alloys for detection of thermal thresholds," IEEE Transactions on Antennas and Propagation, vol. 59, no. 7, pp. 2488–2494, Jul. 2011.

[21] F. Long, X. Zhang, T. Björninen, J. Virkki, L. Sydänheimo, Y.C. Chan and L. Ukkonen. "Implementation and wireless readout of passive UHF RFID strain sensor tags based on electro-textile antennas," in Proceedings of 2015 9th European Conference on Antennas and Propagation (EuCAP), Lisbon, pp. 1-5, 2015.

[22] S. Merilampi, T. Björninen, L. Ukkonen, P. Ruuskanen and L. Sydänheimo, "Embedded wireless strain sensor based on printed RFID tag," Sensor Review, vol. 31, no. 1, pp. 32-40, 2011.

[23] R. Bhattacharyya, C. Di Leo, C. Floerkemeier, S. Sarma, and L. Ananad, "RFID tag antenna based temperature sensing using shape memory polymer actuation," in Proceedings of 2010 IEEE Sensors, Nov, pp. 2363–2368, 2010.

[24] A. A. Babar, S. Manzari, L. Sydanheimo, A. Z. Elsherbeni and L. Ukkonen, "Passive UHF RFID tag for heat sensing applications," IEEE Transactions on Antennas and Propagation, vol. 60, no. 9, pp. 4056-4064, Sept. 2012.

[25] J. Siden, X. Zeng, T. Unander, A. Koptyug and H. Nilsson, "Remote moisture sensing utilizing ordinary RFID tags," in Proceedings of Sensors, 2007 IEEE, Atlanta, pp. 308-311, 2007.

[26] S. Kim, T. Le, M. M. Tentzeris, A. Harrabi, A. Collado and A. Georgiadis, "An RFID-enabled inkjet-printed soil moisture sensor on paper for "smart" agricultural applications," in Proceedings of Sensors, 2014 IEEE, Valencia, pp. 1507-1510, 2014.

[27] S. Sajal, Y. Atanasov, B. D. Braaten, V. Marinov and O. Swenson, "A low cost flexible passive UHF RFID tag for sensing moisture based on antenna polarization," in Proceedings of IEEE International Conference on Electro/Information Technology, Milwaukee, WI, pp. 542-545 , 2014.

[28] D. Shuaib, L. Ukkonen, J. Virkki and S. Merilampi, "The possibilities of embroidered passive UHF RFID textile tags as wearable moisture sensors," in Proceedings of 2017 IEEE 5th International Conference on Serious Games and Applications for Health (SeGAH), Perth, WA, pp. 1-5, 2017.

[29] N. Javed, A. Habib, Y. Amin, J. Loo, A. Akram and H. Tenhunen, "Directly Printable Moisture Sensor Tag for Intelligent Packaging," in IEEE Sensors Journal, vol. 16, no. 16, pp. 6147-6148, Aug.15, 2016.

[30] S. T. Qureshi, T. Björninen and J. Virkki, "Referenced backscattering compression level indicator based on passive UHF RFID tags," in Proceedings of 2018 IEEE International Conference on RFID Technology & Application (RFID-TA), Macau, pp. 1-3, 2018.

[31] X. Chen, L. Ukkonen and T. Björninen, "Passive E-Textile UHF RFID-based wireless strain sensors with integrated references," IEEE Sensors Journal, vol. 16, no. 22, pp. 7835-7836, Nov.15, 2016.

[32] J. Virkki, T. Björninen, S. Merilampi, L. Sydänheimo, and L. Ukkonen, "The effects of recurrent stretching on the performance of electro-textile and screen-printed ultra-high-frequency radio-frequency identification tags," Textile Research Journal, vol. 85, no. 3, pp. 294-301, 2015.